International Conference on Mathematics, Computational Methods & Reactor Physics (M&C 2009)
Saratoga Springs, New York, May 3-7, 2009, on CD-ROM, American Nuclear Society, LaGrange Park, IL (2009)

THE CONVERGED *Sn* ALGORITHM FOR NUCLEAR CRITICALITY

B.D. Ganapol and K. Hadad
Department of Aerospace and Mechanical Engineering
University of Arizona
Ganapol@cowboy.ame.arizona.edu; Hadad@email.arizona.edu

ABSTRACT

A new discrete ordinates algorithm to determine the multiplication factor of a 1D nuclear reactor, based on Bengt Carlson's $\boldsymbol{S_n}$ method, is presented. The algorithm applies the Romberg and Wynn-epsilon accelerators to accelerate a 1D, one-group $\boldsymbol{S_n}$ solution to its asymptotic limit. We demonstrate the feasibility of the ***C***onverged ***Sn*** (***CSn***) solution on several one-group criticality benchmark compilations. The new formulation is especially convenient since it enables highly accurate critical fluxes and eigenvalues using the most fundamental transport algorithm.

Key Words: discrete ordinates, multiplication factor, criticality, one-group

1. INTRODUCTION

The modern era of computational transport theory was ushered in with the discrete ordinates formulation of Wick [1] as implemented by Chandrasekhar [2] in 1950. The elegance of the discrete ordinates method lies in its simplicity enabling computation in multi-dimensions and multi-energies or frequencies. Carlson, in 1953 [3], formulated his version of the discrete ordinates method as a linear interpolation of neutron directions, calling the method the *S*(egment)-*n* method. At that time, the method was particularly suitable for computation as it was fully discretized, stable and second order accurate in space using the so-called diamond difference scheme. Since that time, there have been a multitude $\boldsymbol{S_n}$ methods with extension to multidimensional transport with time for a variety of applications from rarefied gas dynamics to radiative transfer in vegetation canopies and volume rendering for graphics.

Because the $\boldsymbol{S_n}$ method requires full discretization of the spatial and angular variables, discretization error is an integral part of the formulation. Consequently, to obtain an error estimate, one usually performs a sensitivity study to estimate how sensitive the solution is to the chosen discretization. There have been attempts to formalize such an analysis to improve upon the solution [4], but there has been little in the way of a theory based on consistent arguments, until recently [5]. Here, we consider the 1D monoenergetic neutron transport equation to demonstrate an algorithm, based entirely on discretization, to extrapolate to extreme accuracy. In this way, discretized solutions to the transport equation can be optimized to produce self-consistent benchmarks, thus avoiding the need for an independent benchmarking effort altogether.

Here, we use the term extreme accuracy to denote results to 6 or more places. While ultra fine discretized solutions of the transport equation can be made as accurate as desired, we take a sequence acceleration (also called extrapolation) based approach. Rather than discretize spatial

and angular variables in an ad hoc fashion, we choose to use acceleration filters to guide our choice of discretization. It should be emphasized that the value of this work is in the generation of ultra accurate solutions to the transport equation and, in so doing, discovering new numerical algorithms to eventually find use in more comprehensive transport scenarios.

The acceleration method extends the conventional $\boldsymbol{S_n}$ algorithm to benchmark accuracy by redefining what a solution is. The proposed method, called the ***C***onverged ***Sn*** (***CSn***) method, relies on the consistency of the discretized solution to establish the true solution in the limit of zero discretization. Essentially, we accelerate (extrapolate) a sequence of solutions to provide (hopefully) a more accurate one. As will be shown, we realize true acceleration for a variety of 1D critical reactor systems.

Our investigation begins with the establishment of the one-group multiplication factor, *k* for a spatially discretized reactor that simulates criticality when the number of neutrons produced per fission is the physical number divided by *k*. Only where the multiplication factor is one is the reactor truly critical however. We next derive, in a new way, the discretization of the transport equation in both the spatial and angular variables. This leads to the ***Sn*** balance equation, which is our focus and provides the necessary approximations of the multiplication factor to be accelerated to its limit. We then discuss the solution in terms of transport sweeps to avoid full matrix inversion, which is the essence of the ***Sn*** method. Finally, we demonstrate how convergence acceleration gives high accuracy with minimal additional effort.

2. ONE-GROUP THEORETICAL ANALYSIS

In this section, the exact discretization of the one-group transport equation is derived based on interpolation and the Euler-Maclaurin sum formula.

2.1. An Expression for the Multiplication Factor

The transport equation in 1D plane geometry for a slab of width *a* in the one-group approximation with fission and space dependent cross sections is

$$\left[\mu\frac{\partial}{\partial x}+\Sigma(x)\right]\phi(x,\mu)=\frac{1}{2}\sum_{l=0}^{L}\Sigma_{sl}(x)P_l(\mu)\phi_l(x)+\frac{\nu\Sigma_f(x)}{k}\frac{1}{2}\phi_0(x), \qquad (1a)$$

where the Legendre moments are

$$\phi_l(x)\equiv\int_{-1}^{1}d\mu' P_l(\mu')\phi(x,\mu'). \qquad (1b)$$

For isotropic scattering, which we exclusively consider here for demonstration purposes, Eq(1a) becomes

$$\left[\mu\frac{\partial}{\partial x}+\Sigma(x)\right]\phi(x,\mu)=\frac{1}{2}\left[\Sigma_s(x)+\frac{\nu\Sigma_f(x)}{k}\right]\int_{-1}^{1}d\mu'\phi(x,\mu'). \tag{2a}$$

For criticality, we seek the solution subject to zero incoming flux conditions at the medium boundaries

$$\begin{aligned}\phi(0,\mu)&=0\\ \phi(a,-\mu)&=0\end{aligned} \tag{2b}$$

for $\mu>0$. Our objective is to find the multiplication factor k and the corresponding eigenflux $\phi(x,\mu)$.

The solution procedure begins by integration of Eq(2a) over the entire slab to give the following neutron balance in direction μ:

$$\begin{aligned}\mu\left[\phi(a,\mu)-\phi(0,\mu)\right]+\sum_{j=1}^{n}\Sigma_j\int_{x_j}^{x_{j+1}}dx\phi(x,\mu)=\\ =\frac{1}{2}\sum_{j=1}^{n}\left[\Sigma_j+\frac{\nu\Sigma_{fj}}{k}\right]\int_{-1}^{1}d\mu'\int_{x_j}^{x_{j+1}}dx\phi(x,\mu'),\end{aligned} \tag{3}$$

where we assume piecewise smooth cross sections. To perform the spatial integrations in Eq(3), the slab has been partitioned into *n* uniform subintervals $\left[x_j,x_{j+1}\right]$ as shown in Fig. 1.

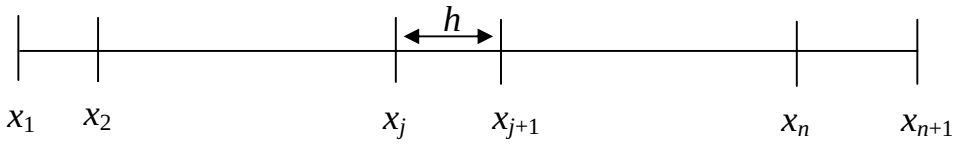

Fig. 1. Uniform spatial discretization

Continuing, we integrate Eq(3) over all directions to give

$$J+\sum_{j=1}^{n}\Sigma_j\int_{x_j}^{x_{j+1}}dx\phi(x)=\sum_{j=1}^{n}\left[\Sigma_j+\frac{\nu\Sigma_{fj}}{k}\right]\int_{x_j}^{x_{j+1}}dx\phi(x), \tag{4a}$$

where the net current exiting the slab is

$$J \equiv \int_0^1 d\mu \mu \left[\phi(a,\mu) + \phi(0,-\mu) \right] = J^+(a) + J^-(0). \tag{4b}$$

We can now simply solve for k

$$k = \frac{\sum_{j=1}^{n} \nu\Sigma_{fj} \int_{x_j}^{x_{j+1}} dx \phi(x)}{\left[J^+(a) + J^-(0) + \sum_{j=1}^{n} \left(\Sigma_j - \Sigma_{sj} \right) \int_{x_j}^{x_{j+1}} dx \phi(x) \right]}. \tag{5a}$$

For a homogenous medium, this expression becomes

$$k = \frac{\nu\Sigma_f \int_0^a dx \phi(x)}{2\int_0^1 d\mu \mu \phi(a,\mu) + (\Sigma - \Sigma_s) \int_0^a dx \phi(x)} \tag{5b}$$

when taking into account the equivalence of the exiting surface currents from symmetry. In what follows, we continue with the homogeneous case.

2.2. The *Sn* Balance Equation

As is quite apparent from Eq(5b), we obtain the multiplication factor only after the flux is known; thus, we must first numerically solve Eqs(2).

Integrating Eq(2a) over the *j*th interval gives

$$\mu \left[\phi(x_{j+1},\mu) - \phi(x_j,\mu) \right] + \Sigma \int_{x_j}^{x_{j+1}} dx \phi(x,\mu) = \int_{x_j}^{x_{j+1}} dx q(x), \tag{6a}$$

where the scattering/fission source is

$$q(x) \equiv \frac{1}{2} \left[\Sigma_s + \frac{\nu\Sigma_f}{k} \right] \phi_0(x). \tag{6b}$$

Assuming a trapezoidal rule for the spatial integrals

$$\int_{x_j}^{x_{j+1}} dx f(x) \approx \frac{h}{2}\left[f\left(x_{j+1}\right) + f\left(x_j\right)\right]$$

gives for Eq(6a)

$$\mu\left[\phi_{j+1}(\mu) - \phi_j(\mu)\right] - \frac{h}{2}\Sigma\left[\phi_{j+1}(\mu) + \phi_j(\mu)\right] = \frac{h}{2}\left[q_{j+1} + q_j\right]. \qquad (7)$$

Since we have now introduced a spatial approximation, the solution is approximated by $\phi_j(\mu)$ for fixed μ and is related to the actual solution through

$$\phi\left(x_j, \mu\right) = \phi_j(\mu) + e_j(\mu) \qquad (8)$$

where $e_j(\mu)$ is the approximation error. We obtain an expression for the error by first integrating Eq(2a) over the slab [0,x_{j+1}] for x_{j+1} fixed

$$\mu\phi_{j+1}(\mu) + \Sigma\int_0^{x_{j+1}} dx\phi(x,\mu) = \int_0^{x_{j+1}} dx q(x).$$

Similarly, summing Eq(7) over the slab

$$\mu\phi\left(x_{j+1},\mu\right) + \Sigma\frac{h}{2}\sum_{j'=1}^{j}\left[\phi_{j'+1}(\mu) + \phi_{j'}(\mu)\right] = \frac{h}{2}\sum_{j'=1}^{j}\left[q_{j'+1} + q_{j'}\right],$$

and subtracting gives

$$\begin{aligned}\mu e_{j+1}(\mu) + \Sigma\left\{I\left[\phi(\mu);0,x_{j+1}\right] - T\left[\phi(\mu);0,x_{j+1}\right]\right\}\left[\phi(\mu);0,x_{j+1}\right] = \\ = \left\{I\left[q;0,x_{j+1}\right] - T\left[q;0,x_{j+1}\right]\right\}.\end{aligned} \qquad (9)$$

In this equation, the terms

$$\begin{aligned} I\left[f;0,x_{j+1}\right] &\equiv \int_0^{x_{j+1}} dx f(x) \\ T\left[f;0,x_{j+1}\right] &\equiv \frac{h}{2}\sum_{j'=1}^{j+1}\left[f_{j'+1} + f_{j'}\right] \end{aligned} \qquad (10)$$

represent an integration over the flux and its trapezoidal rule approximation. Since it is well known from the Euler-Maclaurin formula [6] that

$$I\left[f;0,x_{j+1}\right]-T\left[f;0,x_{j+1}\right]\equiv \\ =-\sum_{k=1}^{\infty}\frac{B_{2k}}{(2k)!}\left\{ f^{(2k-1)}\left(x_{j+1}\right)-f^{(2k-1)}(0)\right\}h^{2k}, \tag{11}$$

upon letting $j\to j-1$ in Eq(9), we find

$$e_j(\mu)=\frac{1}{\mu}\sum_{k=1}^{\infty}\frac{B_{2k}}{(2k)!}\left\{\begin{array}{l}\Sigma\left[\phi^{(2k-1)}\left(x_j,\mu\right)-\phi^{(2k-1)}(0,\mu)\right]- \\ -\left[\Sigma+\frac{\nu\Sigma_f}{k}\right]\int_{-1}^{1}d\mu'\left[\phi^{(2k-1)}\left(x_j,\mu'\right)-\phi^{(2k-1)}(0,\mu')\right]\end{array}\right\}h^{2k}. \tag{12}$$

In Eq(11), B_{2k} is the Bernoulli number. Hence, the error of the spatial discretization is a power series in h^{2k} beginning with h^2.

For the angular discretization, we use the following identity:

$$\phi_j(\mu)=\sum_{m'=1}^{2N}L_{m'}(\mu)\phi_j(\mu_{m'})+\frac{1}{2\pi i}\int_{C_R}dz\frac{P_{2N}(\mu)}{P_{2N}(z)(z-\mu)}\phi_j(z) \tag{13}$$

to define interpolation [6] in the angular variable. Here, $L_m(\mu)$ is the Lagrange polynomial based on the shifted Legendre polynomial of degree $2N, P_{2N}(\mu)$. We specify $2N$ abcissae μ_m to be the zeros of $P_{2N}(\mu)$ and to be symmetric about zero. The contour C_R surrounds the zeros and μ. If

$$\phi_j(\mu_m)=\phi_{j,m}+E_{j,m} \tag{14}$$

is introduced into Eq(7), we find the following discretized balance equation:

$$\left[\mu_m+\frac{h}{2}\Sigma\right]\phi_{j+1,m}-\left[\mu_m-\frac{h}{2}\Sigma\right]\phi_{j,m}= \\ =\frac{h}{4}\left[\Sigma_s+\frac{\nu\Sigma}{k}\right]\sum_{m'=1}^{2N}\omega_{m'}\left[\phi_{j+1,m'}+\phi_{j,m'}\right] \tag{15}$$

and an equation for the angular error

$$\left[\mu_m+\frac{h}{2}\Sigma\right]E_{j+1,m}-\left[\mu_m-\frac{h}{2}\Sigma\right]E_{j,m}= \\ +\frac{h}{4\pi i}\left[\Sigma_s+\frac{\nu\Sigma}{k}\right]\int_{C_R}dz\,\frac{Q_{2N}(z)}{P_{2N}(z)}\left[\phi_{j+1}(z)+\phi_j(z)\right]. \tag{16}$$

Thus in principle, one has an expression for the error which, however, involves the analytical continuation of the flux into the complex plane of the angular variable. From Eqs(8) and (14), we therefore find

$$\phi(x_j,\mu_m)=\phi_{j,m}+E_{j,m}+e_j(\mu_m), \tag{17}$$

where at least a portion of the spatial error behaves like a power series in h^2. We can apply a similar analysis in the negative directions to arrive at the same conclusion of Eqs(12), (16) and (17). Arguments to the effect that the entire error is expressible in a power series of h^2 have also been made [4]. Certainly, for angularly integrated quantities, by virtue of Eq(12), this seems true. . We shall use the error series when we apply convergence acceleration as discussed below.

2.3. Sweeps and Inner Iteration

Equation (15) is most easily solved through iteration by following the particle direction as it passes through the slab from one side to the other and back. With the scattering source assumed known (lagged) in each direction, Eqs(9) are, for $\mu>0$

$$\phi_{m,j+1}^{l+1}=\left[\mu_m+\frac{h}{2}\Sigma\right]^{-1}\left\{\left[\mu-\frac{h}{2}\Sigma\right]\phi_{mj}^{l+1}+\frac{h}{2}\left[q_{j+1}^{l}+q_j^{l}\right]\right\} \tag{18a}$$

and for $\mu<0$

$$\phi_{m,j}^{l+1}=\left[\mu_m-\frac{h}{2}\Sigma\right]^{-1}\left\{\left[\mu+\frac{h}{2}\Sigma\right]\phi_{mj+1}^{l+1}-\frac{h}{2}\left[q_{j+1}^{l}+q_j^{l}\right]\right\}, \tag{18b}$$

where

$$q_j\equiv\frac{1}{2}\left[\Sigma_s+\frac{\nu\Sigma_f}{k}\right]\sum_{m'=1}^{2N}\omega_{m'}\phi_{j,m'}.$$

After the completion of a cycle (one pass back and forth), we update the source for the next inner iteration by

$$q_j^{l+1} \equiv \frac{1}{2}\left[\Sigma_s + \frac{\nu\Sigma_f}{k}\right]\sum_{m'=1}^{2N}\omega_{m'}\phi_{j,m'}^{l+1}. \tag{18c}$$

3. CONVERGENCE ACCELERATION AND STRATEGY

The solution to the balance equations arising from discretization, Eq(15), therefore contains discretization error as shown explicitly by Eq(17). In this section, we discuss the various options for convergence acceleration and an appropriate overall strategy of implementation.

3.1. Romberg Acceleration: Spatial Variable

The key element of the converged ***Sn*** method is extrapolation of the form of the error series expressed in terms of discretization indices to improve the ***Sn*** approximation. Specifically, one uses the form to extrapolate the solution to successive discretizations. For example, consider the determination of the multiplication factor by Eq(5b). In this expression, we require the total neutron content

$$Q \equiv \int_0^a dx\phi(x)$$

which will be the following approximation [from Eqs(8) and (12)]:

$$Q = Q_0(h) + \sum_{k=1}^{\infty}\alpha_k^0 h^{2k}. \tag{19a}$$

where

$$Q_0(h) \equiv \frac{h}{2}\sum_{j=1}^{n}\sum_{m'=1}^{2N}\omega_{m'}\left[\phi_{j+1,m'} + \phi_{j,m'}\right]. \tag{19b}$$

Thus, Q inherits the angular and spatial truncation errors, where the dependence of α_k^0 on quadrature order N is suppressed for now as we consider the error in Q from spatial discretization only (for a fixed N). Equation (19a) becomes

$$Q = Q_0(h) + \alpha_1^0 h^2 + \sum_{k=2}^{\infty}\alpha_k^0 h^{2k} \tag{20a}$$

where Q_0 is the initial approximation to Q of order two. Thus, if we halve h, Eq(20a) becomes

$$Q = Q_0\left(h/2\right) + \alpha_1^0\left[\frac{h}{2}\right]^2 + \sum_{k=2}^{\infty}\alpha_k^0\left[\frac{h}{2}\right]^{2k}. \tag{20b}$$

Now α_1^0 can be eliminated between Eqs(20) to give the improved approximation

$$Q = Q_1\left(h\right) + \alpha_2^1 h^4 + \sum_{k=3}^{\infty}\alpha_k^1 h^{2k}, \tag{21}$$

where the second approximation to Q is

$$Q_1\left(h\right) \equiv \left[\frac{2^2 Q_0\left(h/2\right) - Q_0\left(h\right)}{2^2 - 1}\right],$$

which is of order four. Continuing in this fashion gives the higher order approximations,

$$Q = Q_s\left(h\right) + \alpha_{s+1}^s h^{2(s+1)} + \sum_{k=s+2}^{\infty}\alpha_k^s h^{2k}, \tag{22a}$$

where $Q_s\left(h\right)$, obtained recursively, is

$$Q_s\left(h\right) \equiv \left[\frac{2^{2s} Q_{s-1}\left(h/2\right) - Q_{s-1}\left(h\right)}{2^{2s} - 1}\right] \tag{22b}$$

for $s = 1, 2, \ldots$. This procedure is the well-known Romberg extrapolation [6]. Thus, by refining the grid by multiples of two, we obtain higher order approximations for the content or any quantity derived from the content, like the multiplication factor. Essentially, by successively halving the interval, we are creating a sequence of extrapolations X_s, which we consider converged when

$$e_R \equiv \left|\frac{X_s\left(h\right) - X_{s-1}\left(h\right)}{X_s\left(h\right)}\right| < \varepsilon. \tag{23}$$

X can be k or any flux as long as the sequence is at the same optical depth and direction for all *s* or independent of *x* and μ.

The Romberg extrapolation just described is for a fixed quadrature order *N*. It is well known that a tight coupling exists between space and direction requiring directional refinement along with

spatial refinement for real improvement. Therefore, we next consider convergence of the angular approximation.

3.2. Wynn-Epsilon Acceleration: Angular Variable

Since the intensity, in essence, is a function of the angular quadrature order N, it is a sequence in N that we assume approaches the limit of the true solution. One can therefore apply the Wynn-epsilon (*We*) [7] convergence accelerator to accelerate the sequence to its limit, usually, more quickly than the original sequence. The *We* accelerator takes the following form for the sequence $X_l\left(N_l\right);\ l=0,1,...,L$:

$$\begin{aligned}
&\varepsilon_{-1}^{(l)} \equiv 0 \\
&\varepsilon_{0}^{(l)} \equiv X_l,\ l=0,...,L \\
&\varepsilon_{k+1}^{(l)} = \varepsilon_{k-1}^{(l+1)} + \left[\varepsilon_{k}^{(l+1)} - \varepsilon_{k}^{(l)}\right]^{-1},\ k=0,...,L\ ;\ l=0,...,L-k-1,
\end{aligned} \tag{24a}$$

where X_l is the sequence of the multiplication factors, for example. The recurrence forms a tableau

$$\begin{array}{cccccc}
\varepsilon_0^{(0)} & \varepsilon_1^{(0)} & \varepsilon_2^{(0)} & \cdots & \varepsilon_{L-1}^{(0)} & \varepsilon_L^{(0)} \\
\varepsilon_0^{(1)} & \varepsilon_1^{(1)} & \varepsilon_2^{(1)} & \cdots & \varepsilon_{L-1}^{(1)} & \\
\varepsilon_0^{(2)} & \cdots & & \cdots & & \\
\cdots & & \varepsilon_2^{(L-2)} & & & \\
& \varepsilon_1^{(L-1)} & & & & \\
\varepsilon_0^{(L)} & & & & &
\end{array} \tag{24b}$$

where each element of an even column is an estimate of the desired limit. Convergence comes from interrogation of last term of the even columns $\varepsilon_i^{(L-i)},\ i=0,2,...,2\left[L/2\right]$

$$e_{We} \equiv \left|\frac{\varepsilon_i^{(L-i)} - \varepsilon_i^{(L-i-2)}}{\varepsilon_i^{(L-i)}}\right| < \varepsilon,\ i=2,...,2\left[L/2\right]. \tag{24c}$$

Hence, we vary the angular quadrature through $L+1$ orders N_l to form the sequence to be accelerated by the *We* procedure.

3.3. Acceleration of the Inner Iterations

For the sweeps, a power iteration [8] gives the multiplication factor in the form

$$k_{l+1} = k_l \left[\frac{\sum_{j=1}^{n} \sum_{m'=1}^{2N} \omega_{m'} \phi_{j,m'}^{l+1}}{\sum_{j=1}^{n} \sum_{m'=1}^{2N} \omega_{m'} \phi_{j,m'}^{l}} \right] \tag{25}$$

initiated by $k_0 = 1.5$. Thus, the inner iterations (sweeps) form a sequence for k_l that can also be conveniently accelerated by the *We* acceleration. If we denote the sequence of inner iterations for the multiplication factor by $k_l, l = 0,1,...,R$, the *We* acceleration is Eq(24a) with $N_l = l, L = R.$

3.3. Overall Convergence Strategy

A major advantage of the *We* acceleration, is that we do not require specific knowledge of the error behavior like we do for the Romberg accelerator. This is why it is also possible to apply *We* acceleration to the inner iterations of Eqs(18) to generate an independent sequence also approaching a limit. A second advantage of the *We* acceleration is that little additional programming is required as the acceleration is essentially an "afterthought" that we can apply to any established sequence. For the determination of k to follow however, we consider the accelerations simultaneously with the determination of the original sequence element.

The disadvantage of the *We* acceleration is that a solution is no longer just one discretization and can therefore could be an ensemble of a considerable number of solution elements to achieve the desired convergence. This is the price one gladly pays for higher order accuracy, however.

As should be evident, there are several possible sequences to interrogate for convergence requiring an optimization strategy for most efficiency. Thus, rather than fully converge in either space or direction separately, we follow a "diagonal path" in the (*N*,*n*) discretization space by simultaneously incrementing both discretizations until convergence. Full convergence of the inner iterations at each discretization is required however. In fact, we over converge the inner iterations by several orders of magnitude for best performance incurring an additional, but acceptable cost penalty.

Several sequences therefore present themselves for acceleration. In particular, the original sequence, generated by halving the spatial intervals and incrementing the quadrature order, can be accelerated by *We* as well as Romberg extrapolations. Strictly speaking, however, Romberg acceleration does not apply on a diagonal path in the discretization space, unless convergence results primarily from spatial refinement, which seems to be the case. In addition, we further accelerate the Romberg sequence by *We*. Thus, we will accelerate 3 sequences giving the following convergence possibilities:

(1) the original sequence
(2) the original sequence accelerated by the Romberg acceleration
(3) the original sequence accelerated by the *We* acceleration
(4) the Romberg sequence accelerated by *We* acceleration.

We are now in position to demonstrate the ***CSn*** algorithm.

4. BENCHMARK COMPARISONS

4.1. Comparison to Sood/Forster/Parsons (SFP) Slab Criticality Benchmarks

We first test the converged $\boldsymbol{S_n}$ method on the suit of benchmarks compiled from the literature by A. Sood, A. Forster and K. Parsons [9] in an article entitled *Analytical Benchmark Test Set for Criticality Code Verification.* Table I gives the slab half thicknesses x_c and nuclear properties for 4 homogeneous media criticality benchmarks. The authors designed the benchmarks such that for the data given, the multiplication factor *k* should invariably be unity to five places.

Table I. Single homogenous medium criticality data

Case	x_c	Σ	Σ_f	Σ_s	ν
1)Pu(a)	1.853722	0.3264	0.08160	0.225216	3.24
2)Pu(b)	2.256751	0.3264	0.08160	0.225216	2.84
3)U(a)	2.872934	0.3264	0.06528	0.248064	2.70
4)UD_2O	10.371065	0.54628	0.054628	0.464338	1.70

Tables IIa-d give the multiplication factor k and the relative errors for the four cases. The original and the three accelerated sequences are given. ***N*** and ***n*** give the point along the path in the discretized space. ***Itr*** indicates the number of inner iteration for the converged k at that point. The shaded k-values have converged to better than 5-places. Starting from 4 (2*N*) directions, all accelerated sequences converge to an accuracy of at least 10^{-8} with less than 40 directions and 512 spatial discretizations. For all cases, the accelerated value converged to nearly 3 orders of magnitude better than the original sequence. This clearly shows how convergence acceleration enhances the ***Sn*** method to achieve extreme accuracy. Note that case 1 did not converge to unity as expected indicating, most likely, the half thickness is not as accurate as claimed.

Table III shows the order of the original diamond difference (DD) scheme by assuming the converged value of the multiplication factor as the exact result and forming the expression

$$p = \frac{\ln\left(\left|k - k_{DD}(h)\right|\right) - \ln\left(\left|k - k_{DD}(h/2)\right|\right)}{\ln 2}.$$

As observed, the correct order is captured to 4 places, which is indeed a sensitive test of convergence acceleration.

Table IIa. Case 1

N	*n*	*Ori*	*We*	*Rbg*	*We/Rbg*
2	2	9.66034E-01	9.66034E-01	9.66034E-01	9.66034E-01
4	4	9.88658E-01	9.88658E-01	9.96200E-01	9.96200E-01
6	8	9.97196E-01	1.00237E+00	1.00030E+00	1.00086E+00
8	16	9.99293E-01	9.99976E-01	9.99984E-01	1.00003E+00
10	32	9.99822E-01	1.00000E+00	9.99999E-01	1.00000E+00
12	64	9.99954E-01	9.99998E-01	9.99998E-01	9.99998E-01
14	128	9.99987E-01	9.99998E-01	9.99998E-01	9.99998E-01
16	256	9.99995E-01	9.99998E-01	9.99998E-01	9.99998E-01

Relative Error

N	*Itr*	*Ori*	*We*	*Rbg*	*We/Rbg*
2	4	1.00000E+00	1.00000E+00	1.00000E+00	1.00000E+00
4	8	2.28839E-02	2.28839E-02	3.02809E-02	3.02809E-02
6	10	8.56145E-03	1.36792E-02	4.09671E-03	4.65545E-03
8	9	2.09898E-03	2.39356E-03	3.13449E-04	8.28028E-04
10	8	5.29022E-04	2.36809E-05	1.48620E-05	3.02226E-05
12	8	1.31919E-04	1.92170E-06	1.08978E-06	2.89961E-06
14	7	3.29898E-05	9.68178E-08	6.39398E-08	4.75885E-08
16	7	8.23912E-06	8.41131E-09	1.40377E-08	7.48707E-09

Table IIb. Case 2

N	*n*	*Ori*	*We*	*Rbg*	*We/Rbg*
2	2	9.64512E-01	9.64512E-01	9.64512E-01	9.64512E-01
4	4	9.88107E-01	9.88107E-01	9.95973E-01	9.95973E-01
6	8	9.97032E-01	1.00246E+00	1.00028E+00	1.00087E+00
8	16	9.99255E-01	9.99993E-01	9.99991E-01	1.00003E+00
10	32	9.99814E-01	1.00000E+00	1.00000E+00	1.00000E+00
12	64	9.99953E-01	1.00000E+00	1.00000E+00	1.00000E+00
14	128	9.99988E-01	1.00000E+00	1.00000E+00	1.00000E+00
16	256	9.99997E-01	1.00000E+00	1.00000E+00	1.00000E+00

Relative Error

	Itr	*Ori*	*We*	*Rbg*	*We/Rbg*
2	4	1.00000E+00	1.00000E+00	1.00000E+00	1.00000E+00
4	9	2.38792E-02	2.38792E-02	3.15875E-02	3.15875E-02
6	10	8.95068E-03	1.43172E-02	4.30147E-03	4.88935E-03
8	11	2.22512E-03	2.46709E-03	2.84122E-04	8.33907E-04
10	8	5.58975E-04	8.64734E-06	9.50380E-06	2.97102E-05
12	8	1.39573E-04	1.30879E-06	6.08765E-07	2.50735E-06
14	8	3.49009E-05	1.72344E-07	3.71380E-08	3.33387E-08
16	7	8.71593E-06	1.48990E-08	1.47821E-08	7.47598E-09

Table IIc. Case 3

N	*n*	*Ori*	*We*	*Rbg*	*We/Rbg*
2	2	9.56811E-01	9.56811E-01	9.56811E-01	9.56811E-01
4	4	9.86172E-01	9.86172E-01	9.95959E-01	9.95959E-01
6	8	9.96489E-01	1.00208E+00	1.00019E+00	1.00060E+00
8	16	9.99120E-01	1.00002E+00	9.99999E-01	1.00002E+00
10	32	9.99780E-01	1.00000E+00	1.00000E+00	1.00000E+00
12	64	9.99945E-01	1.00000E+00	1.00000E+00	1.00000E+00
14	128	9.99986E-01	1.00000E+00	1.00000E+00	1.00000E+00

Relative Error

N	*Itr*	*Ori*	*We*	*Rbg*	*We/Rbg*
2	4	1.00000E+00	1.00000E+00	1.00000E+00	1.00000E+00
4	10	2.97727E-02	2.97727E-02	3.93068E-02	3.93068E-02
6	10	1.03526E-02	1.58715E-02	4.23174E-03	4.63994E-03
8	11	2.63349E-03	2.05612E-03	1.93452E-04	5.80891E-04
10	9	6.60276E-04	1.99257E-05	1.70201E-06	1.99266E-05
12	8	1.65071E-04	7.45301E-07	1.55600E-07	1.25629E-06
14	8	4.12556E-05	2.13822E-08	1.43753E-08	1.26627E-08

Table IId. Case 4

N	*n*	*Ori*	*We*	*Rbg*	*We/Rbg*
2	2	9.61405E-01	9.61405E-01	9.61405E-01	9.61405E-01
4	4	9.91413E-01	9.91413E-01	1.00142E+00	1.00142E+00
6	8	9.97893E-01	9.99678E-01	9.99962E-01	1.00005E+00
8	16	9.99474E-01	9.99984E-01	9.99998E-01	9.99997E-01
10	32	9.99868E-01	1.00000E+00	9.99999E-01	9.99999E-01
12	64	9.99967E-01	1.00000E+00	1.00000E+00	1.00000E+00
14	128	9.99992E-01	1.00000E+00	1.00000E+00	1.00000E+00
16	256	9.99998E-01	1.00000E+00	1.00000E+00	1.00000E+00
18	512	9.99999E-01	1.00000E+00	1.00000E+00	1.00000E+00

Relative Error

N	*Itr*	*Ori*	*We*	*Rbg*	*We/Rbg*
2	4	1.00000E+00	1.00000E+00	1.00000E+00	1.00000E+00
4	15	3.02678E-02	3.02678E-02	3.99539E-02	3.99539E-02
6	17	6.49369E-03	8.26738E-03	1.45351E-03	1.37037E-03
8	21	1.58151E-03	3.05951E-04	3.54724E-05	4.78164E-05
10	23	3.94513E-04	1.63703E-05	1.97980E-06	2.10084E-06
12	25	9.89836E-05	3.10282E-07	5.46911E-07	8.29827E-07
14	15	2.47490E-05	1.36056E-07	3.97186E-08	1.79782E-07
16	13	6.17330E-06	1.07484E-07	1.99185E-08	1.51978E-08
18	12	1.55798E-06	2.74089E-08	2.29723E-08	8.49694E-09

We hope to continue to test all benchmarks in the Sood, *et al*. suit in the future. This will include anisotropy, heterogeneity and spherical geometry.

Table III. Variation of diamond difference order with discretization

h	*p*
5.1855E+00	-8.9134E+00
2.5928E+00	2.0261E+00
1.2964E+00	2.0003E+00
6.4819E-01	1.9994E+00
3.2410E-01	1.9992E+00
1.6205E-01	1.9999E+00
8.1024E-02	2.0000E+00
4.0512E-02	2.0000E+00

4.2. Comparison to Kaper, Lindeman and Leaf (KLL) Benchmarks

One of the first high fidelity eigenvalue benchmark compilations was authored by H. Kaper, A. Lindeman and G. leaf, entitled *Benchmark Values for the Slab and Sphere Criticality Problem in One-Group Neutron Transport Theory* [10]. There, the authors solve the integral transport equation using singular eigenfunctions. In a rather involved derivation, an iteration emerges which is anything but straightforward. The numerical evaluations involve *X*-functions and seem to require a significant amount of numerical tuning. For our comparison, we must convert the *k* evalulation to yield *c*, which is given iteratively as

$$c_{l+1}(a) = c_l(a)\left[\frac{\sum_{j=1}^{n}\sum_{m'=1}^{2N}\omega_{m'}\phi_{j,m'}^{l}(a)}{\sum_{j=1}^{n}\sum_{m'=1}^{2N}\omega_{m'}\phi_{j,m'}^{l+1}(a)}\right]$$

and, on convergence, forms the function

$$f(a) = c - c(a)$$

as input to a bisection procedure to find the value *a* that makes $f(a) = 0$. Table IVa shows

Table IVa. Comparison to KLL Benchmark

c	*a*
1.01E+00	8.32951356E+00
1.02E+00	5.66550546E+00
1.05E+00	3.30026377E+00
1.10E+00	2.11330967E+00
1.20E+00	1.28937928E+00
1.30E+00	9.37725554E+00
1.40E+00	7.36603551E-01
1.60E+00	5.11962989E-01
2.00E+00	3.11025906E-01

the multiplication factor found by the ***CSn*** algorithm. The highlighted values are in disagreement with these of Table I of the KLL compilation. A recent set of benchmark values produced by S. Loyalka (SKL) [11] using the numerical procedure of KLL, but evaluating with multiple precision computer algebra, are given in Table IIIb. In comparison to these results, all

Table IVb. Comparison to SKL Benchmark

c	*a*
1.01E+00	8.329513561E+00
1.02E+00	5.665505456E+00
1.05E+00	3.300263772E+00
1.10E+00	2.113309666E+00
1.20E+00	1.289379285E+00
1.30E+00	9.377255543E-01
1.40E+00	7.366035510E-01
1.60E+00	5.119629886E-01
2.00E+00	3.110259059E-01

digits but one are in agreement with the ***CSn*** values indicating that the discrepancies in Table IVa are associated with the KLL values. The digits highlighted in Table IVb are in disagreement with those of the SKL compilation. The excellent agreement of the ***CSn*** with a presumably more accurate and sophisticated evaluation, which however requires multiple precision arithmetic, highlights the simplistic nature of the diamond difference formulation and the genius of Bengt Carlson.

5. CONCLUSION

We have shown that the simple and straightforward ***Sn*** method perfected nearly 50 years ago can be reformulated to give benchmark accuracy through the ***CSn*** algorithm. By wrapping several convergence accelerations around the ***Sn*** algorithm, one obtains up to 10 digits of accuracy for k-eigenvalues. The convergence accelerations are the Romberg and Wynn-epsilon accelerations, which are mathematically based to accelerate a sequence more quickly to its limit. The Romberg accelerator requires knowledge of the error behavior; while, the *We* accelerator does not. We have demonstrated the ***CSn*** algorithm on several standard bare critical reactors as a first proof of principle. While we anticipated superior behavior in plane geometry, the real challenge will be spherical geometry.

REFERENCES

1. G.C. Wick, Uber Ebene Diffusionsprobleme, *Z. Phys*. **121**,702 (1943).
2. S.A. Chandrasekhar, *Radiative transfer*, Oxford Press, London, 1950.
3. B.G. Carlson, Solution of the transport Equation by S_n Approximations, LA-1599, Los Alamos Scientific Laboratory (1953) and rived in LA-1891 (1955).
4. E. Allen, Application of Richardson's Extrapolation to the Neutron Transport Equation, *NS&E*, **99**, 123-133 (1988).
5. B.D. Ganapol and D.E. Kornreich, Mining the Multigroup-Discrete Ordinates Algorithm for High Quality Solutions, *ANS M&C Topical*, Avignon, 2005.
6. P.J. Davis, P. Rabinowitz, *Methods of Numerical Integration*, Academic Press, MA (1984).
7. G. Baker, P. Graves-Morris, *Padé Approximants*, Cambridge University Press, NY (1996).

8. E. Lewis and W.F. Miller, Jr., Computational Methods of Neutron Transport, ANS Publications, Lagrange Park Il, 1993.
9. A. Sood, A. Forster, A. and K. Parsons, Analytical Benchmarks Test Set for Criticality Code Verification, *Prog., in Nucl. Ener*., **42**, 55(2003).
10. H. Kaper, A. Lindeman and G. leaf, Benchmark Values for the Slab and Sphere Criticality Problem in One-Group Neutron Transport Theory, *NS&E*, **54**, 94-99 (1974).
11. S. Naz and S. Loyalka, Some Benchmarks Results on Criticality of a Slab, *ANS Trans*. **95**, 591-593, Nov.2006.